

Interactive comment on “Mechanism of Seasonal Arctic Sea Ice Evolution and Arctic Amplification” by K.-Y. Kim et al.

K.-Y. Kim et al.

kwang56@snu.ac.kr

Received and published: 28 June 2016

Interactive comment on “Mechanism of Seasonal Arctic Sea Ice Evolution and Arctic Amplification” by K.-Y. Kim et al.

Anonymous Referee #2 Received and published: 30 May 2016

This study applies a novel technique (Cyclostationary empirical orthogonal function analysis) to ERA-interim reanalysis to examine physical processes behind Arctic sea ice reductions and Arctic amplification. While the study is unique and has the potential to yield insight on causal mechanisms, a number of issues should be addressed before publication.

Comment1(C1): The CSEOF technique requires a more broad-based description, in-

Printer-friendly version

Discussion paper



cluding how the approach differs from standard EOF analysis, interpretation of the results in Table 1, how the spatial and temporal components of Figure 2 were derived, and the impact of mode 1 explaining only 15% of the total variability.

Response1(R1): We modified the “method of analysis” section significantly in order to address what the reviewer requested including the definition and interpretation of R2 value. This section should be much clearer now. [P4 L7- P6 L13]

The spatial patterns and temporal components of Figure 2 (in manuscript) are the result of CSEOF analysis. They are B_1 (r,t) and T_1 (t) of 2m air temperature.

The leading mode explains ~15% of the total variability of 2 m air temperature. In other words, 85% of the variance of surface air temperature variability derives from other mechanisms. This is something that we cannot control; it is the nature of our climate system. Since temperature variability associated with Arctic amplification explains only ~15% of the total variability, it is all the more important to separate it from other mechanisms of variability. Otherwise, temperature variability associated with Arctic amplification will be obscured seriously by variability from other sources, and an accurate physical and statistical inference of Arctic Amplification would be difficult. We also want to say that this mode is well separated from the second CSEOF mode (Arctic oscillation; Kim, K.-Y. and Son, S.-W.: Physical characteristics of Eurasian winter temperature variability, Environ. Res. Lett., 11, 044009, 2016.).

C2: Throughout the manuscript, the term ‘sea ice melting’ is used to describe what are essentially negative winter (DJF) sea ice concentration anomalies in the Kara/Barents sea with a maximum value of -10% (Figure 3). I’m not convinced this is the correct terminology to use. The negative ice concentration anomalies in this region are impacted in some combination by the timing of sea ice formation and temperature anomalies during the ice growth season (thermodynamics) and potential changes in ice motion and advection during the winter (dynamics). This may be semantics, but to refer to winter season negative ice concentration anomalies as ‘ice melting’ does not seem

appropriate to me.

R2: We used the terminology ‘sea ice melting’ in order to address sea ice loss from the perspective of Arctic amplification. As you mentioned, however, melting is not the only means of sea ice reduction. Therefore, we changed ‘sea ice melting’ to ‘sea ice loss’ or ‘sea ice reduction’ except when we really meant ‘melting’. [correction scatted in the manuscript]

C3: Related to the point above, all of the analysis is based on ERA-interim reanalysis, including sea ice concentration. This raises some questions: -how is ERA-interim sea ice concentration derived? Has it been validated? How does it compare to the more widely used passive microwave sea ice concentration data records? -how sensitive is this analysis to the choice of sea ice information? Do the results differ if sea ice information independent of the ERA-interim atmospheric fields is used?

R3: Sea ice concentration (SIC) in the ERA-Interim data is an estimate from other operational products such as operational NCEP product and sea surface temperature and sea ice analysis (OSTIA). These products are based on passive microwave satellite measurements (Donlon et al. : The Operational Sea Surface Temperature and Sea Ice Analysis (OSTIA) system, Remote Sens. Environ., 116, 140-158, 2012). In order to confirm that the results in the present study are not sensitive to the sea ice concentration dataset, CSEOF analysis was conducted on a different sea ice concentration dataset acquired from National Snow & Ice Data Center (NSIDC at nsidc.org). The specific dataset used is “sea ice concentration from Nimbus-7 SSMR and DMSP SSM/I-SSMIS Passive Microwave data”, which is generated from brightness temperature data. The data are provided in the polar stereographic projection at a grid cell size of 25 x 25 km. We used the data in 1990-2014, since there are a large number of missing points in earlier data.

Figure R1 is the regressed patterns of sea ice concentration for the first (Arctic Amplification) CSEOF mode derived from the NSIDC dataset in comparison with that derived

Printer-friendly version

Discussion paper



from the ERA-Interim data. As can be seen in the figure, there is no serious discrepancy between the two datasets. Both the spatial pattern and magnitude of variation in sea ice concentration in conjunction with the Arctic Amplification mode is quite similar between the two. The R^2 value of regression is 0.97 for the first CSEOF mode, suggesting that the amplitude of variation of the sea ice patterns in Figure R1 is physically consistent with the Arctic warming patterns in Figure 2 in the manuscript. [no corrective action]

C4: What is the source of the sea surface temperature data?

R4: Sea surface temperature of ERA-Interim reanalysis data has been used in the present study. As a comparison between Figures R3 and R4 shows, the SSTA patterns derived from the ERSST data are not much different from those of ERA-Interim reanalysis data in terms of the key features. We used the ERA-Interim SST in order to maintain physical consistency among the variables analyzed in the present study. [no corrective action]

C5: I understand the general idea behind calculating the ‘sea ice melting mechanism’ (Figure 9) in terms of feedbacks associated with a given sea ice concentration change. A 1% sea ice concentration change, however, is not really physically relevant. This is well within the error of ice concentration datasets, and sea ice doesn’t really change in this manner. This feedback totally discounts the role of ice dynamics – ice doesn’t simply sit in one place and respond to temperature anomalies with an increase or decrease in ice concentration.

R5: As the reviewer pointed out, sea ice loss is not entirely due to melting and ice dynamics certainly was not accounted for in this discussion. What we are referring to is an average picture of physical change due to sea ice loss. As explained in the method section, regression in CSEOF space allows us to write data in the form:

$$\text{Data}(r,t) = \sum_n \{B_n(r,t), C_{reg_n}(r,t), D_{reg_n}(r,t), E_{reg_n}(r,t), \} T_n(t),$$

[Printer-friendly version](#)
[Discussion paper](#)


where the terms in curly braces for each n represents a physical process as reflected in different variables (say, temperature, sea ice concentration, 850 hPa air temperature, upward longwave radiation, etc.). The terms in curly braces are physically consistent with each other. For example, Figure R5 below shows the daily evolution associated with the Arctic Amplification mode. CSEOF analysis was conducted on the daily ERA-Interim data during winter (Dec. 1-Feb. 28), and the first CSEOF mode represents Arctic Amplification as in the present analysis. Shown in Figure R5 are the terms in curly braces for five different variables averaged over the Barents-Kara Seas [21° - $79.5^{\circ}\text{E} \times 75^{\circ}$ - 79.5°N]. As can be seen in the figure, loss of sea ice is reflected in the positive values of anomalous 2 m air temperature, 850 hPa temperature, upward longwave radiation, and downward longwave radiation. Daily variations of atmospheric variables are highly correlated with each other, suggesting that they have a common cause (see Figure R6). Specifically, the impact of synoptic disturbance is conspicuous with significant fluctuations on synoptic time scales.

Further, CSEOF analysis indicates that these variations are amplifying in time as reflected in the PC time series in Figure R5(d). The mechanism described in Figure 9 is the winter average picture of the mechanism shown in Figure R5. We can average the CSLVs in Figure R5 during winter to estimate the relative magnitude of change in heat flux or atmospheric variables as sea ice loss continues. Whatever the cause of sea ice reduction is, a 1% loss of sea ice results in the changes in other variables as described in Figure 9. Further, the lagged correlation analysis among these variables indicates that turbulent heat flux precedes 850 hPa warming, which, in turn, is followed by increased downward longwave radiation (see Figure R6). Ultimately, surface air temperature increases due to increased downward longwave radiation.

On the other hand, the mechanism addressed above cannot be demonstrated in CSEOF analysis of monthly data. The cause-and-effect relationship among the variables in Figure R5 can only be appreciated when we analyze 3-hourly data. Therefore, we remove the entire discussion associated with Figure 9. Hopefully, we will address

[Printer-friendly version](#)[Discussion paper](#)

this mechanism in a new paper where 3-hourly data is employed for CSEOF analysis.
[Removed the text associated with Figure 9.]

* Figure Captions

Figure R1. The Arctic Amplification mode of NSIDC sea ice concentration

Figure R2. The Arctic Amplification mode of ERA-Interim sea ice concentration

Figure R3. The regressed seasonal patterns of ERA-Interim sea surface temperature (shading; 0.05 K) and the reduction of sea ice concentration (contours; 2 %) in the Arctic region (64.5°-90° N).

Figure R4. The regressed seasonal patterns of ERSST (shading; 0.05 K) and the reduction of sea ice concentration (contours; 2 %) in the Arctic region (64.5°-90° N).

Figure R5. Daily patterns of variability over the region of sea ice loss (21°-79.5°E × 75°-79.5°N): (a) sea ice concentration, (b) 2 m air temperature (red), 850 hPa air temperature × 2 (black), and upward longwave radiation (blue), and (c) same as (b) except for the regressed downward longwave radiation (blue). Correlation of upward and downward longwave radiations with 2 m air temperature is respectively 0.90 and 0.95, whereas with 850 hPa air temperature is 0.60 and 0.86. (d) Corresponding PC time series.

Figure R6. Correlation of upward (solid lines) and downward (dotted lines) longwave radiations with 2 m air temperature (blue), 850 hPa temperature (red), and sea ice concentration (black). Longwave radiation lags the other variable for a positive lag. Lagged correlation between 2 m air temperature and 850 hPa air temperature (black dashed line); 2 m air temperature leads 850 hPa temperature for a positive lag.

** The combined response file including a marked-up manuscript is attached.

Please also note the supplement to this comment:

<http://www.the-cryosphere-discuss.net/tc-2016-69/tc-2016-69-AC2-supplement.pdf>

Interactive comment on The Cryosphere Discuss., doi:10.5194/tc-2016-69, 2016.

TCD

Interactive
comment

Printer-friendly version

Discussion paper



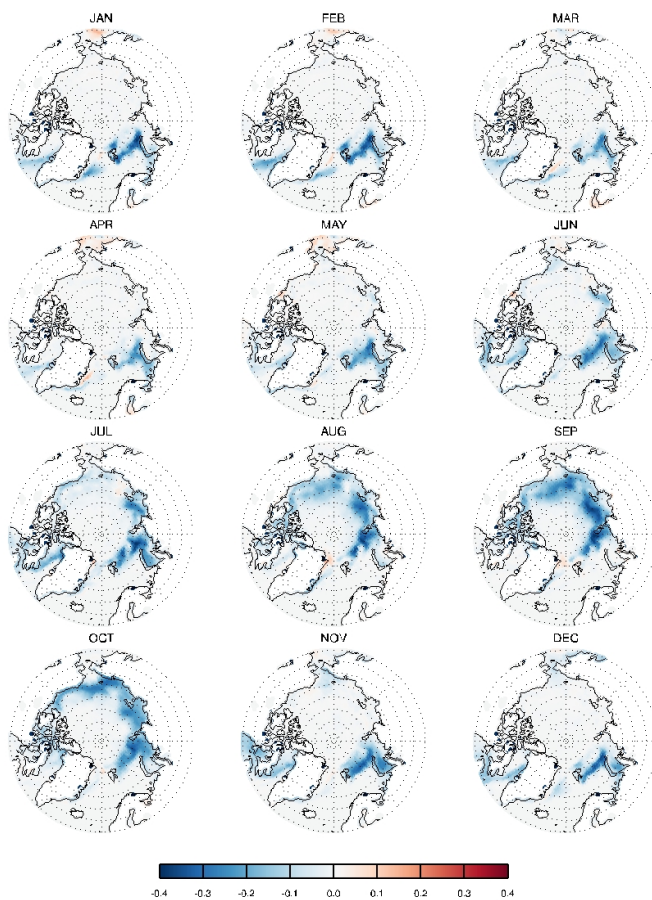


Fig. 1. The Arctic Amplification mode of NSIDC sea ice concentration

[Printer-friendly version](#)[Discussion paper](#)

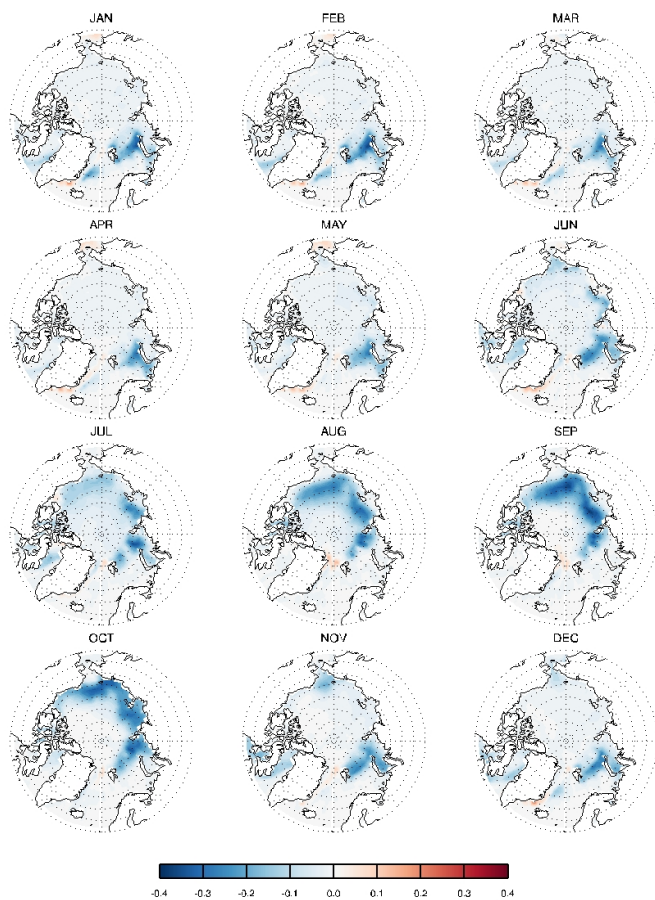


Fig. 2. The Arctic Amplification mode of ERA-Interim sea ice concentration

[Printer-friendly version](#)[Discussion paper](#)

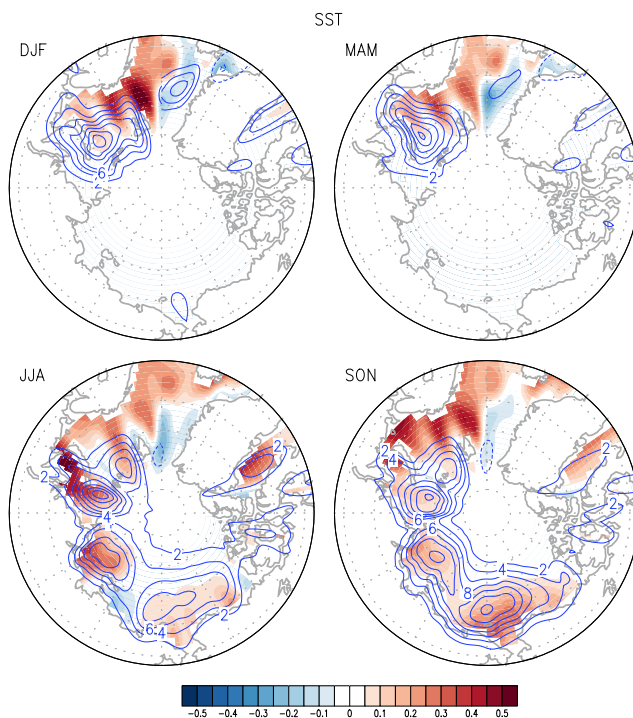


Fig. 3. The regressed seasonal patterns of ERA-Interim sea surface temperature (shading; 0.05 K) and the reduction of sea ice concentration (contours; 2 %) in the Arctic region (64.5°-90° N).

[Printer-friendly version](#)[Discussion paper](#)

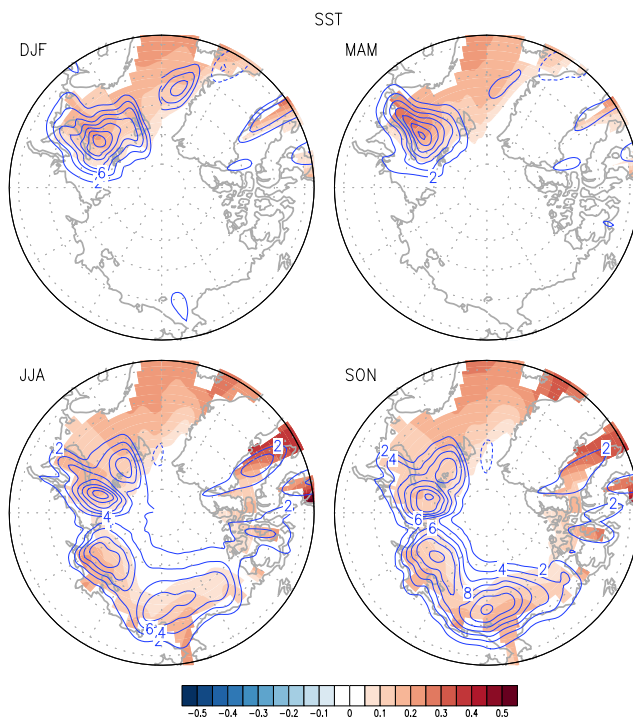


Fig. 4. The regressed seasonal patterns of ERSST (shading; 0.05 K) and the reduction of sea ice concentration (contours; 2 %) in the Arctic region (64.5°-90° N).

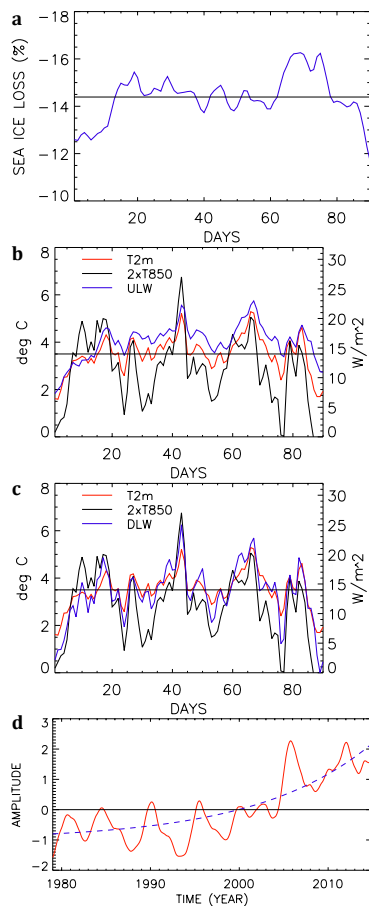


Fig. 5. Daily patterns of variability over the region of sea ice loss (21°-79.5°E × 75°-79.5°N): (a) sea ice concentration, (b) 2 m air temperature (red), 850 hPa air temperature × 2 (black), and upward longw

Printer-friendly version

Discussion paper



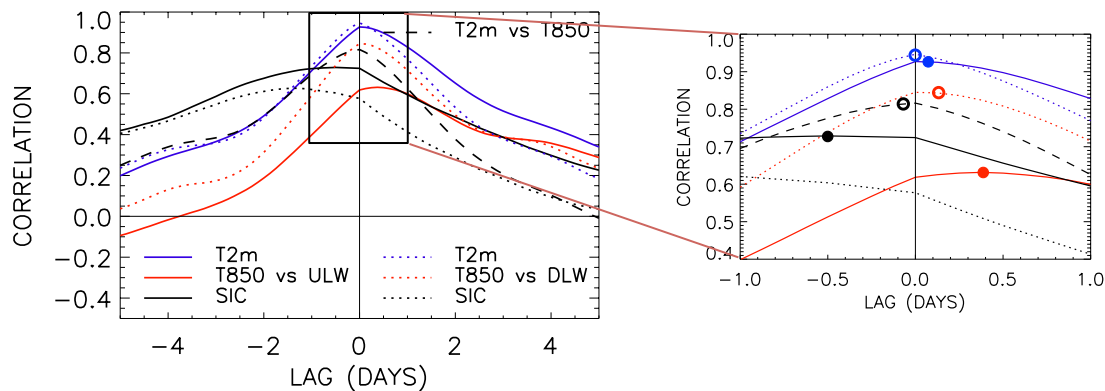


Fig. 6. Correlation of upward (solid lines) and downward (dotted lines) longwave radiations with 2 m air temperature (blue), 850 hPa temperature (red), and sea ice concentration (black). Longwave radiation I

[Printer-friendly version](#)[Discussion paper](#)